e-ISSN 2320 –7876 www.ijfans.org
Vol.11, Iss.9, Dec 2022

Research Paper

INFLUENCE OF THE THE INTERPLANETARY MAGNETIC FIELD STRENGTH ON THE PROPERTIES OF MAGNET ON SHEATH MIRROR MODES

KRISHNAVENI.P
Research Scholar
M.Phil Physics
Bharath Institute Of Higher Education And Research
Mail Id : krishnaveni2329@gmail.com

Dr.K.THIYAGARAJAN
Head of the Department, Department Of Physics
Bharath Institute Of Higher Education And Research

Address for Correspondence
KRISHNAVENI.P
Research Scholar
M.Phil Physics
Bharath Institute Of Higher Education And Research
Mail Id : krishnaveni2329@gmail.com

ABSTRACT

Magnet has a profound influence on human life even before it was identified as a separate state of matter. From clinical to mechanical, it has given us countless possibilities to make our lives easier. Apart from celestial magnet, nearly all the laboratory magnets involve surface interactions. The interaction process is a complicated process. The high energetic ions from the bulk magnet are most likely to hit the surface, resulting in dislocation of the surface atoms. The process is characterized as *sputtering*. In due course of time, sputtering can lead to a situation where the atoms from the surface start coming out, leaving behind voids in the material.The situation is described as *erosion*. The sputtered atoms can be ionized and enter thebulk magnet resulting in contamination. It brings some serious concern about the lifetime of the magnet as well as the material that contains it. The fundamental properties of magnet ensure that whenever a external is unprotected to themagnet, a thin layer of stimulating particles is developed to safeguard the electric field createdby the surface. The charged layer is known as *Debye Sheath*. The sheath is consideredas the critical region to solve the majority of the issues faced by the magnet community in surface interaction. The region is responsible for the acceleration of charged particlestowards the surface. Introducing oblique magnetic field in the system provides further control over the process. Smaller angle efficiently reduces the energy of the incoming particles. The presence of magnetic field brings in an additional layer along with the *Debye Sheath*, named as *Chodura Sheath* or *Magnetic Presheath*. In contrast to the electrostatic case, the potential drop in the magnetized magnet takes place across the *Chodura Sheath* and

e-ISSN 2320 –7876 www.ijfans.org
Vol.11, Iss.9, Dec 2022

Research Paper

Debye Sheath jointly.

INTRODUCTION

In the visible universe, 99.9% of the matter is in a state called magnet[1], a significant topic of discussion in the science community. In search of unlimited clean energy, the whole humankind is running after fusion, which is considered viable only in the magnet environment. Unlike the sun, it is quite challenging to confine magnet inside a laboratory. Various attempts have been made to make fusion a reality, but only a few have shown anticipation.

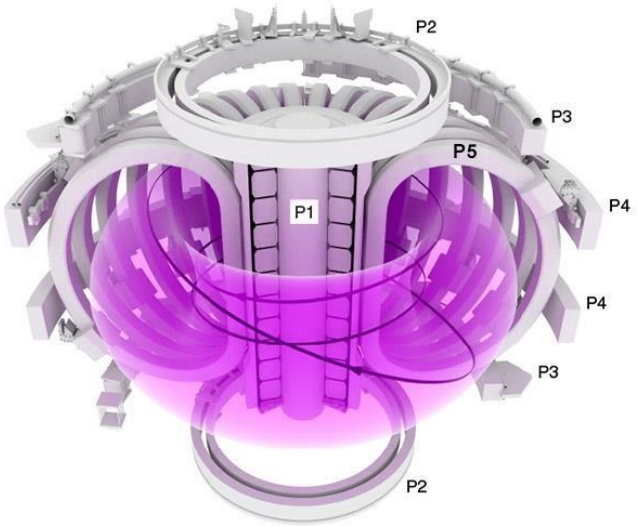

Fig. 1.1 The electromagnetic coil arrangement at the Joint European Torus (JET). (P1) is the Centralsolenoid provides the magnet current, (P2-P4) are the shaping magnets, and (P5) is the toroidal magnets. (Source: EUROfusion)

Whatever measures we take into, the charged particles are prone to touch thesurface of the vessel because of centrifugal force. The event where the surface is exposed to magnet leaves a substantial impact on both the magnet and the surface. Whileenergetic magnet particles often erode the surface by sputtering, the sputtered atoms canalso enter the bulk magnet resulting magnet contamination[3]. The importance of magnet surface interaction in fusion leads us to study the fundamental physics involvingthe control parameters of the whole process, in due course, which will help us to reducethe effect of such events.

Different Approaches to Study Magnet

Comprising of charged particles and neutrals makes magnet the most difficult mediumto

study. The movement of the charged particles is easily affected by any external electric or magnetic field, which eventually leads to more complex particle trajectory. Even in the absence of any external field, the self-generated fields produced by charged particle movement is enough to make the system unpredictable. Therefore, to study such complex system keeping the physics intact, some approximations are required. The following two approaches are exceptionally well accepted among magnet physicists to explore the different properties and processes in magnet: the macroscopicapproach and the microscopic approach. Now, each has its merit and demerits. In the midst of various macroscopic methods, the fluid approach is considered as the most relevant. In case of microscopic approach, there are two widely used approaches: the kinetic and the statistical.

1.1.1 Fluid Approach

The idea of fluid modeling was conceptualized from the fluid mechanics. Instead of studying the individual particle movement, the motion of the fluid element is considered here. The very idea of fluid modeling is based on the fact that the particles in the fluid element are bound together by the persistent collisions among themselves. To use such notion in magnet (being a collection of charged particles) a few assumptions are taken into account. First, the inter-particle collisions in the system are considered independent of any macroscopic field to ensure an equilibrium velocity distribution of charged particles. The velocity distribution of each species is commonly assumed as Maxwellian where everything is determined by only two parameters density and temperature[6]. Secondly, the movement of the fluid element represents the average particle motion in the system. The macroscopic fields are considered as an outcome of the fluid element movement. In a magnet system, the continuity and momentum equations of a fluid element are expressed as follows:

The continuity equation for a species can be written as,

$$\frac{\partial n}{\partial t} + \boldsymbol{\nabla} \cdot (n\boldsymbol{v}) = S \qquad (1.3)$$

The momentum equation for the same species can be written as,

$$mn\left(\frac{\partial \boldsymbol{v}}{\partial t} + \boldsymbol{v} \cdot \boldsymbol{\nabla} v\right) = (\boldsymbol{E} + \boldsymbol{v} \times \boldsymbol{B}) - \boldsymbol{\nabla} p + \boldsymbol{F} \qquad (1.4)$$

e-ISSN 2320 –7876 www.ijfans.org
Vol.11, Iss.9, Dec 2022

Where n represents the number density of the species, v represents the velocity of the same. S represents source term. $\boldsymbol{\nabla} p$ and $\boldsymbol{F}$ represents pressure gradient force and general force in the system. q, m, $\boldsymbol{E}$, and $\boldsymbol{B}$ have their usual meaning. The pressure forces in the macroscopic equations of a fluid element originates from the spatial variation of distribution functions of the charged particles[7].

Kinetic Approach

(a) Phase Space

The Phase space is a representation of the instantaneous dynamic state of each particle in a system[4]. In Cartesian coordinate, phase space is described in a six-dimensional space (x, y, z, v_x, v_y, v_z) consisting of velocity and space. For a single particle system, the phase space is called as μ-space and for a system with many particles is referred as Γ-space. For a system of particles, a point in the Γ-space represents a single microscopic state.

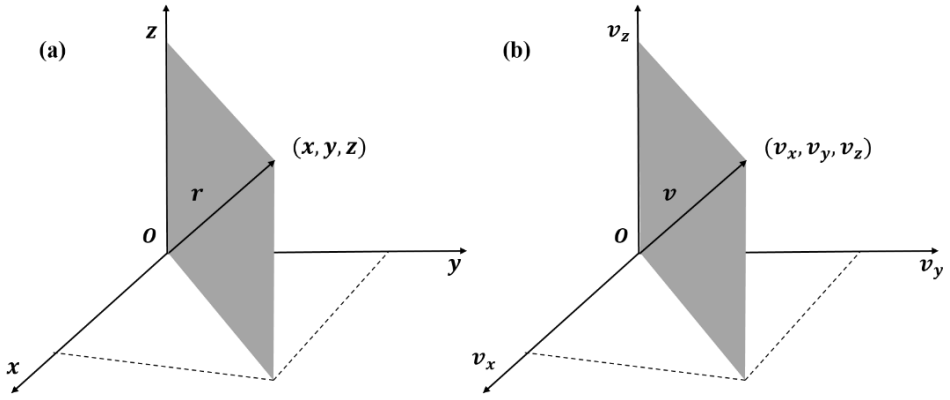

Fig. 1.2 Position vectors in (a) configuration space and (b) velocity space. (Source: J. A. Bittencourt[4])

From the distribution function of a system, one can get to know whether a magnet is homogeneous, inhomogeneous, isotropic or anisotropic. If the function does not dependent on space vector ($\boldsymbol{s}$) of the system, the system can be referred as homogeneous(e.g., magnet at an equilibrium state). In a reverse situation, the system is described as inhomogeneous. Likewise, in velocity space, if the function varies with the orientation of the velocity vector ($\boldsymbol{v}$), it is called as an anisotropic system. In contrast, if it onlydepends on the magnitude, is referred as isotropic.

In kinetic theory, one of the primary objectives is to deduce the distributionfunction for an individual system.

(b) Number Density

The number density ($\boldsymbol{s}, t$) is a macroscopic variable for a system which represents the number of particles per unit volume in a configuration space. The expression for number density can be written as,

$$(\boldsymbol{s}, t) = \frac{1}{d^3 s} \iiint_{v} d^6(\boldsymbol{s}, \boldsymbol{v}, t) \qquad (1.13)$$

Using equation (1.12), the number density can be expressed as,

$$(\boldsymbol{s}, t) = \iiint_{v} (\boldsymbol{s}, \boldsymbol{v}, t)\, d^3 v \qquad (1.14)$$

The integral used in the expression of number density over velocity space represents integration over each velocity component (v_x, v_y, v_z) ranging from $-\infty$ to $+\infty$.

1.1.1.1 Boltzmann Equation

Apparently, this proves that any velocity component under equilibrium has a Gaussian distribution.

e-ISSN 2320 –7876 www.ijfans.org
Vol.11, Iss.9, Dec 2022

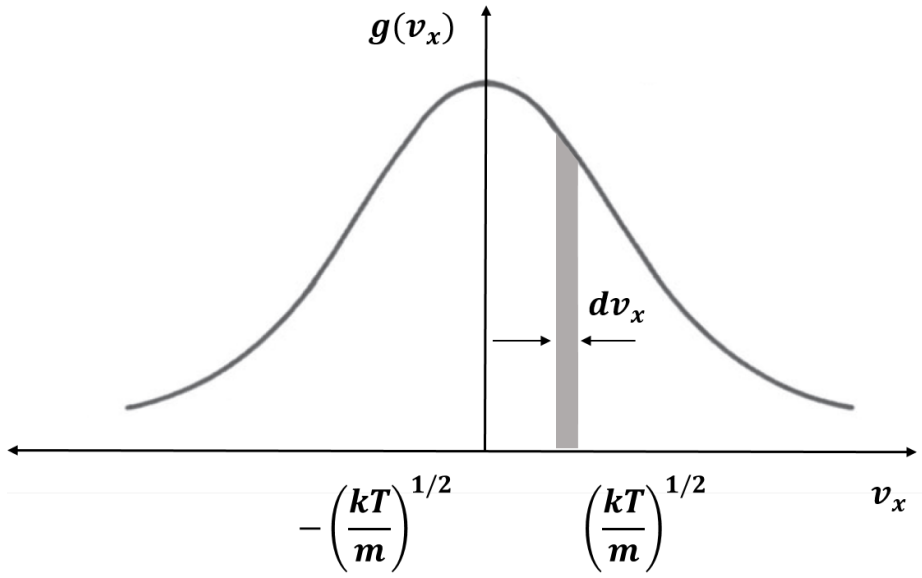

Fig. 1.3 At equilibrium Maxwellian distribution function for each velocity component takes the Gaussian shape.(Source: J. A. Bittencourt[4])

1.1.2 Particle in Cell (PIC) Approach

Particle in Cell (PIC) approach is unique. It provides kinetic material by subsequentthe routes of a big amount of separate particle. Hence, it is referred as the microscopic approach to study magnet. Like other kinetic approaches, it does not deal with particle distribution directly. To track trajectories, it solves Maxwell's equations for charged particles in the system. Particle in Cell was initially developed to study low-density magnet as it takes immense computation power to track individual particles in a magnet. Moreover, at low-density magnet is less likely to behave as a single fluid. It becomes a collection of discrete charged particles and neutrals. To study magnet in thepresence of external or self-induced magnetic fields with inter-particle collisions is quite tricky. It becomes more difficult to calculate when we attempt to solve realistic

scenarios. In practical mostly systems are bound and there are different surfaces and object inside a system. In which case the traditional methods are not suitable to study such systems. Particle in Cell approach gives the tool to overcome the problems we face in the earlier methods. Although, it brings a different set of issues to the scene. Particle in Cell method can be classified into two categories: Electrostatic PIC (ES- PIC) and

e-ISSN 2320 –7876 www.ijfans.org
Vol.11, Iss.9, Dec 2022

Electromagnetic PIC (EM-PIC). In the ES-PIC method, it is considered that the current generated by the magnet is small enough to ignore the self-induced magneticfield. This assumption reduces Maxwell's equations to simpler ones resulting in less computation. Particles in magnet move with different characteristic time scale according to their masses. For example, being the lighter species electrons move muchfaster as compared to heavy ions. Considering electrons to follow Boltzmann relation,the time scale of calculation can be done in more extended periods (as per ion time scale). It also helps to reduce the particle noise in the phase space for the ions in the system. Although, it is not mandatory in ES-PIC to consider electrons as Boltzmann distributed if there is enough computation power available. In EM-PIC, the self-inducedmagnetic field comes into the picture, and the particles movement is tracked by solving full Maxwell's equations. In this thesis, the problems are tackled with ES-PIC considering no self-induced magnetic field. Although, there is a static external magneticfield in the system which has been handled by using particle rotation in the movementphase (Section d). Therefore, we will keep our introduction limited to electrostatic cases.

(a) Interpolation of Fields to Particles

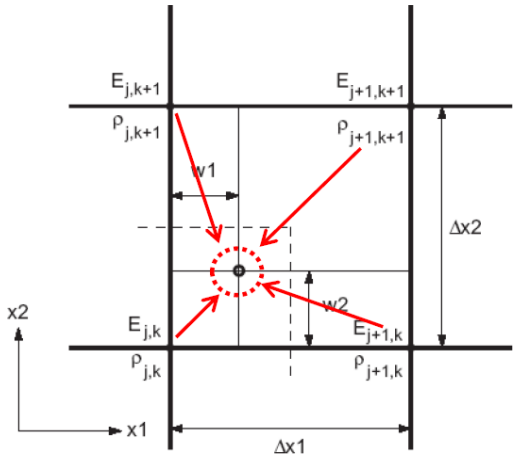

Fig. 1.7 Schematic diagram of field interpolation to a charge in a 2D cell.

We have calculated our fields at the nodes while particles are inside the cell. Now to get the force acting on individual particles the integrated fields are interpolated

e-ISSN 2320 –7876 www.ijfans.org
Vol.11, Iss.9, Dec 2022

(weighted) to the particle positions in a reverse mechanism carried out in the section – a.

The electric field applied to the particle will be the vector sum of all the electric field contribution at the particle location ($x1$, $x2$). Similarly, magnetic fields and other quantities are weighted onto the particle positions as per requirement.

(b) Integration of Equations of Motion

The movement of charged particles in magnet is oversaw by Lorentz force. In the previous step, the force acting on individual particles are computed. Now, using Newton's law of motion, we can perform the integration of particle motion through time step Δt. The usually used addition technique is leapfrog technique. In the leapfrog method, first the velocity is integrated through the time step and then the position is updated. The method is referred as leapfrog because the velocity and positions integrated with an offset of half a time step ($\Delta t/2$).

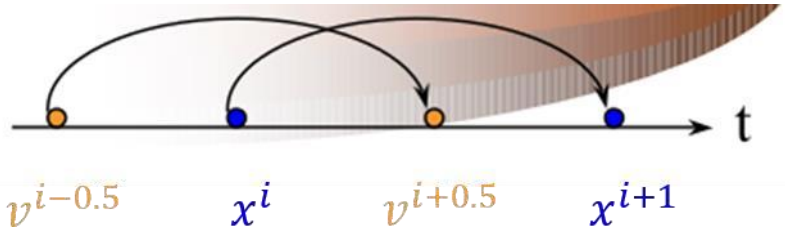

Fig. 1.8 Schematic of Leapfrog method. (Source: Jeff Hammel)

The finite difference representation of the scheme is written as,

$$v^{i+0.5} = v^{i-0.5} + \frac{q}{m} E\Delta t \qquad —$$

$$x^{i+1} = x^i + v^{i+0.5}\Delta t \qquad (1.29)$$

If there is an applied magnetic field that should also be included in the expression given above.

(c) Particle Loss/Gain at the Boundaries

After performing a particle push (integration of equations of motion), it is essential to

confirm that all the particle are in the computational domain. If any particle reaches the boundary (end of computational domain), the particle is handled then according tothe nature of the boundary. Primarily boundaries in magnet systems are three types: reflective, absorptive, and emissive. For a reflective boundary, macroparticles are addressed by a velocity reversal, for absorptive boundary particles are just destroyed as soon as they reach the boundary. In case of an emissive boundary, which often happens in case of sputtering or secondary emission events (details in Section – 1.4), a new species is added to the simulation according to the surface interaction physics.

- **The Knudsen Number**

The gas thermalization is governed by the collision process, the rate of which inversely varies with the gas density. The critical parameter in collisional magnet is the mean free path (λ_{mfp}), the average distance travelled by a molecule between consecutive collision.

$$\lambda_{mfp} = \frac{1}{\sigma n} \quad (1.30)$$

Where σ is the collision cross-section, n is the number density of the gas molecules. The expression for the Knudsen number can be written as,

$$Kn = \frac{\lambda_{mfp}}{L} \quad (1.31)$$

e-ISSN 2320 –7876 www.ijfans.org
Vol.11, Iss.9, Dec 2022

If the collision mean-free-path in a system is way smaller than the system length ($\lambda_{mfp} \ll L$), the system can be modeled using fluid approach (continuum flow). In a complete reverse case i.e. $\lambda_{mfp} \gg L$, the system is best described by free molecular flow[14]. In a specific situation where collisions are highly infrequent i.e. $\lambda_{mfp} \sim L$ (e.g., rarefied gas) kinetic approaches are considered to be the best practice. However,kinetic methods can also be used to study continuum flow if the huge requirement of computational power is supplied.

1.2 Magnet Sheath

At the beginning of this thesis, we have discussed three fundamental properties of magnet. One of which is Debye shielding, the phenomena to shield any local electric field appeared inside a magnet system. Now consider a magnet system of positively charged ions and electrons bounded between two surfaces. Usually, the electrons possess higher thermal velocity ($\sqrt{eT_e/m_e}$) in compared to the ions ($\sqrt{eT_i/m_i}$) due to their low mass and high temperature. Due to the high thermal velocity electrons, they reach the surface first and make it negative. The quasi-neutrality property of magnet ensures that in such case positively charged ions rush towards the surfaces and shield the electric field appeared due to the electrons. As a result, a positive space charge layer is formed in front of the surface, which is referred as Sheath or Debye Sheath. The width of the non-neutral sheath region is generally a few electron Debye length.

e-ISSN 2320 –7876 www.ijfans.org
Vol.11, Iss.9, Dec 2022

Research Paper

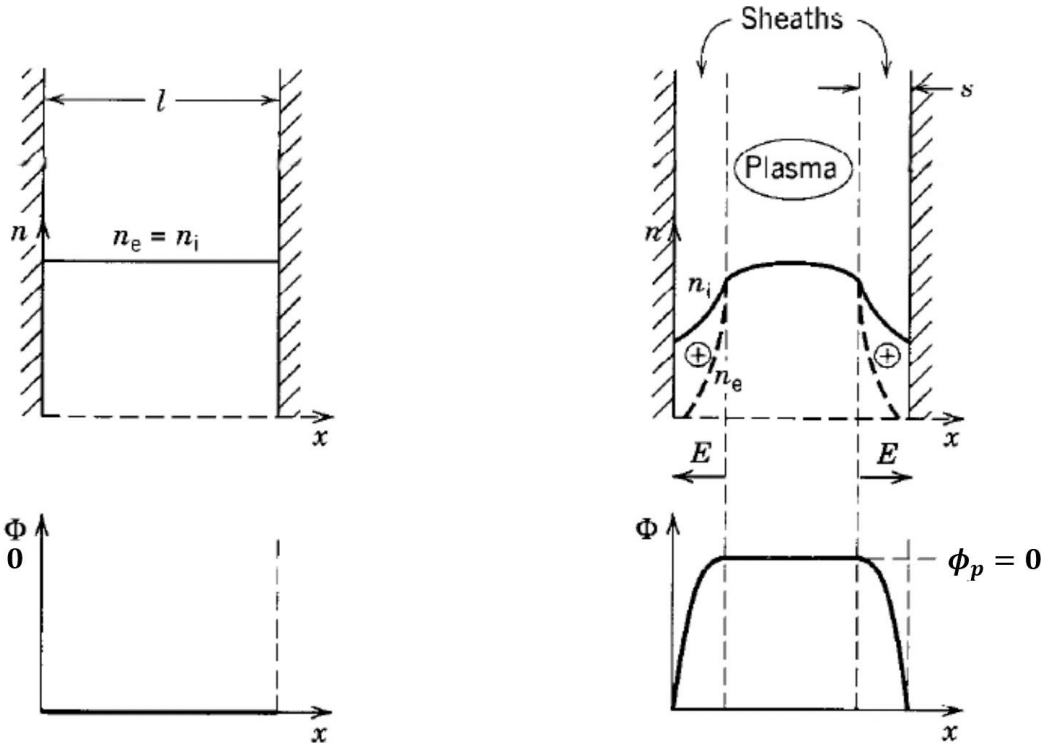

Fig. 1.9 Formation of the magnet sheath. (Credit: Lieberman et al.[7])

Due to the potential gradient created by electrons, ions are enhanced near the external. The ions need to attain a minimum velocity (of the order of $\sqrt{kT_e/m_i}$, considering ~~$T_e \gg T_i$~~) before entering into the sheath to shield the electric field produced by electrons, which is described as the Bohm criterion[15]. The Bohm criterion is considered to be a mandatory condition (which is debatable) to form a stable sheath in weakly ionized magnets. The minimum velocity at which ions enter into the sheath region is referred as Bohm velocity.

e-ISSN 2320 –7876 www.ijfans.org
Vol.11, Iss.9, Dec 2022

Research Paper

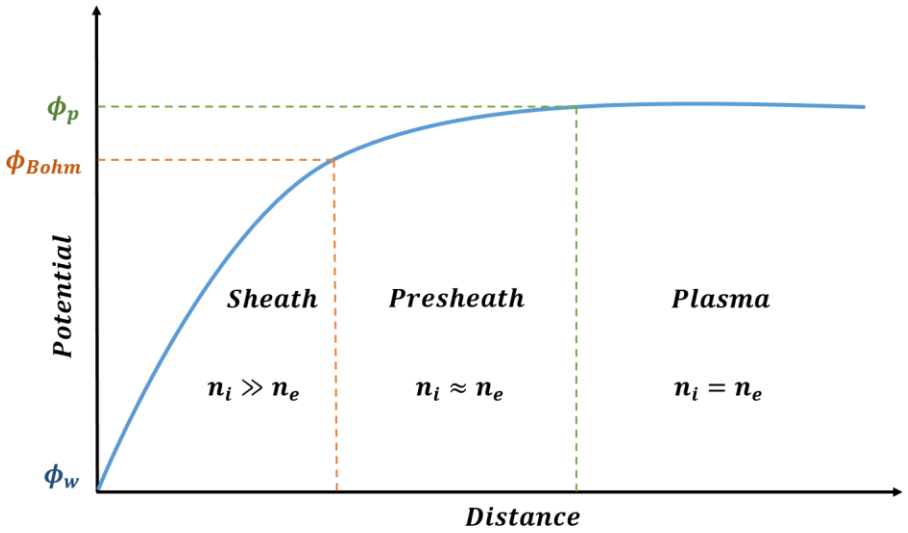

Fig. 1.10 Schematic diagram of magnet sheath potential and its different regions.

Magnet sheath is a non-linear problem. However, with some proper assumptions, we can solve it keeping the physics intact. Let us contemplate a 1D magnet system with zero ion temperature (T_i = 0) and drift velocity (along with the x-axis) towards the wall as

u_0 at the sheath entrance. To get a steady state solution of a collisionless sheath, we also have to shoulder that the electrons are Boltzmann distributed. The magnet potential (x) is a monotonically decreasing solution.

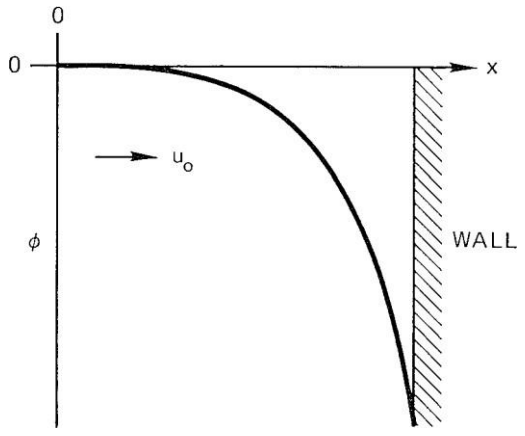

Fig. 1.11 Potential in a planar sheath. Cold ions are assumed to have uniform velocity u_0 at the sheathentrance. (Credit: F. F. Chen[16])

e-ISSN 2320 –7876 www.ijfans.org
Vol.11, Iss.9, Dec 2022

e

$\sqrt{(m_i)}$

The expression (1.38) represents the non-linear solution of a planar sheath.

In addition to the space charge sheath, there is another region, which is responsible for accelerating ions to the Bohm velocity, named as presheath, a quasi-neutral region. At the border among presheath and cover, ions make a transition from subsonic to supersonic regime[7]. The ion dynamics in the presheath and sheath region is not as simple as it seems. There are plenty of factors to make the scenario different. For example, a collision can play a huge role in altering ion velocity in the presheath which eventually forbids it to satisfy Bohm criterion[17].

1.2.1 Magnetized Magnet Sheath

In the presence of an external magnetic field, the particles in front of a surface behave in a completely different way than the electrostatic case. If the applied magnetic field is parallel to the particle motion, it does not create any difference in the analysis. However, a system where the applied external magnetic field makes an angle (acute) with the surface present in front of the magnet, in addition to presheath and sheath, a new region is developed, named as magnetized presheath or Chodura Sheath (CS) [18].

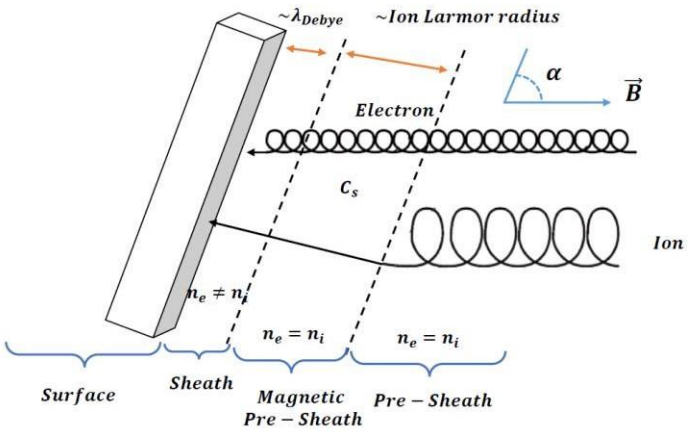

Fig. 1.12 Schematic diagram of a magnetized sheath and its different regions.

The CS is considered as a quasi-neutral region of few ion Larmor radii thickness sandwiched between the two-layer presheath and sheath. Although CS is quasineutral, it contains some electric field, which is responsible for turning the ion flow from parallel magnetic field direction to the direction perpendicular to the wall (see Fig. 1.12).

The inclusion of magnetic field in the scenario does not necessarily mean the primary condition to form the sheath is violated. The Debye sheath region is minimal compared to the presheath and does not depend on the magnetic field at all. Hence, the Bohm criterion is also considered as one of the primary condition here (except for a few individual cases).

1.2.1.1 Brief Summary of the Researches Done in the Field

In 1982, Chodura first reported the existence of the magnetized presheath layer in the presence of oblique magnetic field using a fluid model[18]. Later in 1994 Riemann studied the same stressing on the effect of collision in the presheath region[19]. In this particular work, Riemann used a single integral equation, which provides the solution for the velocity component perpendicular to the surface. The technique is entirely different from the method of solving momentum equations simultaneously. His work proves that the presence of active magnetic field efficiently compresses the collisional presheath. In 1995, Stangeby came up with a new theoretical model of presheath-sheath transition for ions[20]. In his work, he concluded that the ion flow velocity at the sheath edge must be equal or higher than sonic (Bohm criterion) even in the presence of magnetic field. He also added that at the magnetic presheath entrance the velocity component parallel to B must be equal or higher than sonic which is commonly referred as the Chodura criterion. In 1997, Ahedo found that magnetic field strength and the angle of incidence has a substantial impact on the Chodura layer[21].

1.3 Sputtering and Surface Erosion

When an energetic ion (atom) collides with a surface, it first transmits its momentum to a target atom known as the primary knock-on atom (PKA)[33]. The incident atom may either come to rest in thermal equilibrium with the target (implantation) and then lose momentum in a future collision, or it can be reflected off the target (backscattering). Within the target material, the PKA causes a collision cascade. Some of the atoms may reach the target's surface as a result of the cascade process. In the event that the

e-ISSN 2320 –7876 www.ijfans.org
Vol.11, Iss.9, Dec 2022

When atoms reach the surface and have more energy than the target material's surface binding energy, they break away from the surface (physical sputtering). Other methods include chemical sputtering and radiation assisted sublimation, in addition to physical sputtering., which have quite an essential role in the sputtering process. However, these processes are dependent on the surface material that is exposed to the magnet. For example, if the surface is carbon based and the magnet contains hydrogen,then most likely chemical sputtering will take place due to its active hydrocarbon formation tendency. In this thesis, we have kept ourselves limited to the materials that only involves physical sputtering.

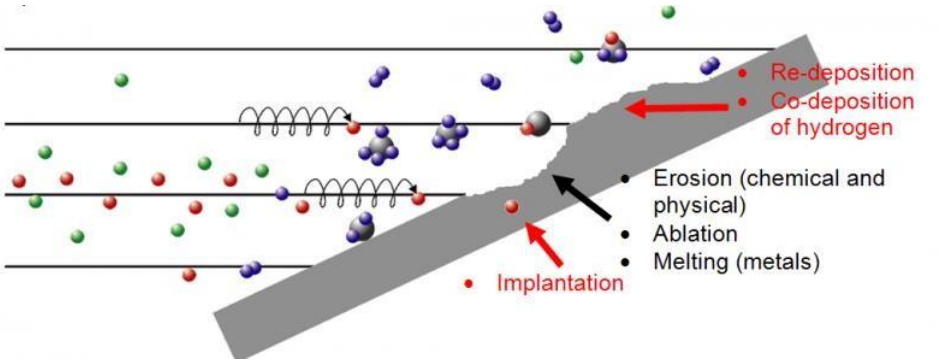

Fig. 1.13 In a tokamak geometry, field lines intersect the divertor plate with a small angle. Charged particles follow the field lines in a helical path and strike the surface (divertor) resulting sputtering anderosion processes. (Source: G. Manfredi)

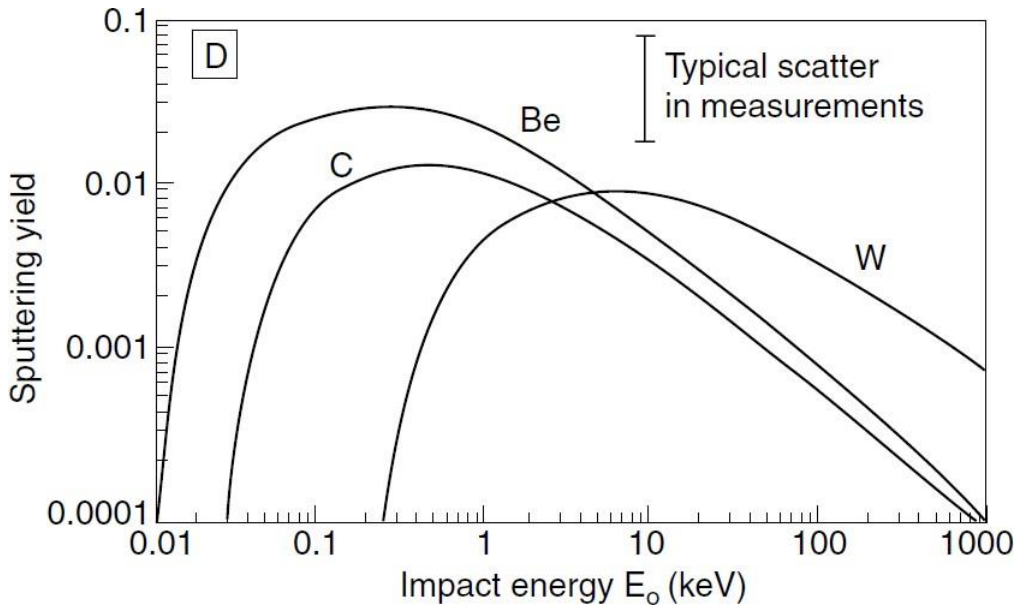

e-ISSN 2320 –7876 www.ijfans.org
Vol.11, Iss.9, Dec 2022

Fig. 1.14 Physical sputtering yields for D on Be, C and W surfaces for normal incidence, calculated using the TRIMSP code. (Source: P. C. Stangeby[3])

where Q and the threshold energy E_{th} are appropriate limits, E_0 is the event subdivision vigor (eV). S_n is the atomic discontinuing cross-section founded on the Kr-C potential and approximated as,

$$S_n(\epsilon) = \begin{cases} \dfrac{0.5}{\ln(1+1.2288g)} \\ \dfrac{}{g+0.1728g^{\frac{1}{2}}+0.008g^{0.1504}} \end{cases} \quad (1.48)$$

$\epsilon = E_0/E_{TF}$ is the abridged energy and E_{TF} is the Thomas-Fermi energy (eV). The look for ϵ is as follows,

$$\epsilon = E_0 \frac{M_2}{M_1+M_2} \frac{a_L}{Z_1 Z_2 e^2} \quad (1.49)$$

Z_1, Z_2 and M_1, M_2 are the projectile's nuclear charge and the target's atomic mass, respectively. The electron charge is e, while the Lindhard screening length is aL.

e-ISSN 2320 –7876 www.ijfans.org
Vol.11, Iss.9, Dec 2022

1 1
2 2 2
9π2 3

a_L = (—) a_B (Z^3 + Z^3) (1. 50)

128 1 2

where, a_B is the Bohr radius.

The look for popping yields (1.47) later on modified by Eckstein et. al.[35] dueto unforeseen yields underneath a verge value. The new fit formulation is given by

E_0 μ
(−1)
$Y^{phy}(E\ ) = QS$ $(\epsilon)\frac{E_{\text{th}}}{}$ (1. 51)

0 n E_0 μ

λ+(−1)
E
th

where λ and μ are fitting parameters.

Now for oblique occurrence, the fit formulation was given by Yamamura et al.[36] and lateron was adapted by the same group as,

Y^{phy} $(E_0, \theta) = Y_{ph}(E_0, 0)$ {cos [(π c − f × exp {b (1 − $\frac{1}{\theta\ \pi\ c}$)} (1. 52)
y]}

0 2 cos[(θ_{02})]

Equation (1.52) is almost identical to Yamamura et al. except for the inclusion of extra physical information, a binding energy Esp, which causes an incident atom to accelerate and refract towards the surface normal to prevent parallel incidence (= 90°). The expression for 0 is as follows:,

$$\theta_0 = \pi - \arccos \frac{1}{\sqrt{1+\frac{E_0}{E_{sp}}}} \geq \frac{\pi}{2} \quad (1.53)$$

For noble gas E_{sp} is considered as zero and for hydrogen isotopes $E_{sp} = 1\ eV$ is expected. The only issue with the new data is, it delivers fitting parameters for Tungsten within a incomplete range of impact dynamisms. Consequently, to estimate the

e-ISSN 2320 –7876 www.ijfans.org
Vol.11, Iss.9, Dec 2022

Popping for tall temperature relations, one has to select a dissimilar variety of electron temperatures.

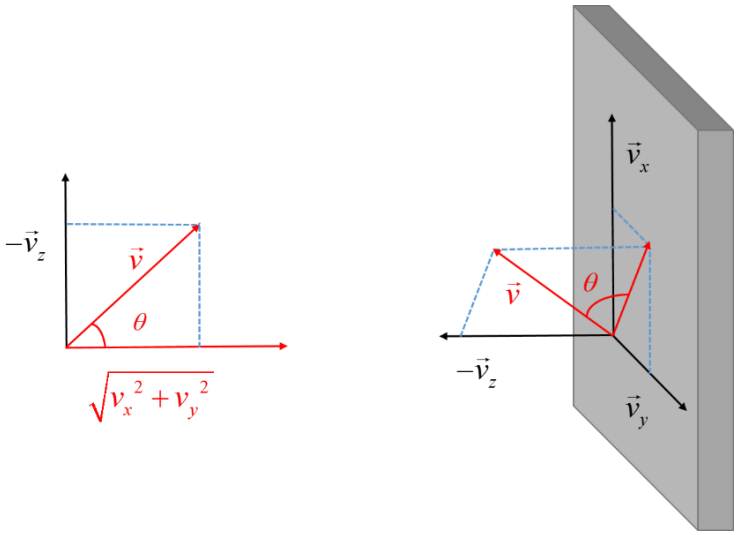

Fig. 1.15 Schematic of θ calculation.

We utilised the algorithm for estimating physical sputtering yield from Warrier et alearlier .'s work[33]. The original subroutine has been changed to utilise as part of the post-processing phase of the main theoretical work, according to the new empirical fit formula provided by equation (1.52). The values for the various fitting parameters were obtained from the most recent report from the IPP in Germany[37]. The subroutine's formula is correct for ions colliding with a monoatomic target. In the current computations, we have also evaded the self-sputtering and redeposit ion marvels. We have presented our method of gauging the incidence angle () of ions in Fig. 1.15. The angle is calculated using the formula below.:

$$\theta = \arctan\left(\frac{v_z}{\sqrt{v_x^2+v_y^2}}\right) \quad (1.54)$$

e-ISSN 2320 –7876 www.ijfans.org
Vol.11, Iss.9, Dec 2022

The angle θ used here is totally dissimilar from the angle α mentioned in the earlier sections.

1.4 Motivation

In nuclear fusion devices,[38] divertor plays a crucial role in impurity control as it receives highest power thicknesses[39] from the core magnet. Divertors are eroded by ionand neutral bombardment, which affects their lifetime, as well as produce impurity. Theuse of beryllium, carbon, and tungsten as magnet-facing materials (PFMs) in ITER callsfor dedicated investigations on their behavior under the expected particle and power loads and neutron irradiation. To optimize the heat load and erosion the design of divertor and choice of material is critical. It is essential to study the magnet surface interaction process in the edge region to keep this two factor within reasonable limits,. While laboratory experiments in fusion devices are indispensable to test their integral performance, theoretical modeling provides the basis for the understanding of the fundamental properties and the behavior of edge magnets.

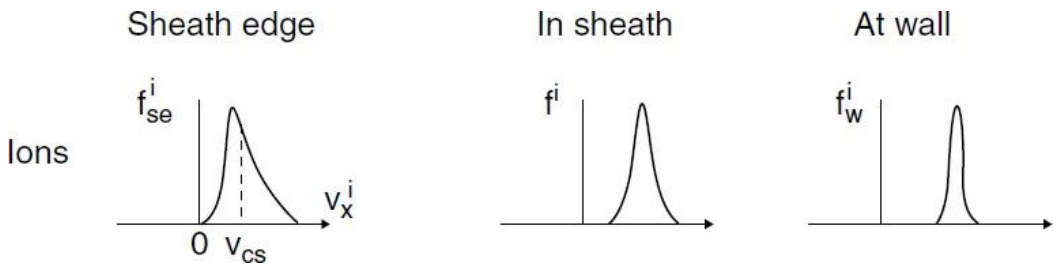

Fig. 1.16 The velocity distribution functions for ions at the sheath edge, in the sheath, and at thewall/surface. At sheath, edge ions deviate from Maxwellian distribution due to the presheath acceleration to satisfy Bohm criterion. (Source: R. Chodura)

In magnetized magnet devices like tokamaks, the field lines are incredibly complicatedleaving particle trajectories unpredictable. In the edge region where the surface meets the hot magnet, it is imperative to get a detailed picture of how the ions get affected. The militaries manipulating the ion subtleties in the sheath must be unstated to gain a broad insight of the sheath structure. Issues like the inflection of the sheath leading toperturb dissimilar magnet parameters in the core magnet are quite significant. In the presence of sheath, the particle distribution deviates from a Maxwellian[40] causing instabilities. Such problems can only be clarified by learning the leading forces that control the ion dynamics, which made us pursue our first study.

ADYNAMICANALYSIS OF THE MAGNETIZEDSHEATH

In this chapter, we have attempted to analyze the ion dynamics in the presence of an oblique magnetic field. The transport process in the sheath is quite complicated. The involvement of magnetic forces makes the process more intricate. A numerical simulation has been performed to study such system using fluid approach. The outcomeof this study is quite significant for surface interaction study. It has been observed thation momentum is shared among different components while there is no collision in thesystem. Mimicking single particle motion, we have also tried to study the flowvelocities of ions to extract more delicate information.

Results and discussions

2.1.1 Variation of the angle α

The electric field in this article is along the z-axis, and the ions are supposed to flow towards the wall thanks to the combined effect of the electric and magnetic fields. Let's have a look at how angle variation impacts ion dynamics as a whole. The development of the electric potential and electric field down the z-axis is shown in figures 2.2 and 2.3. These values may be used to estimate sheath thickness. The length of the sheath seems to shrink as the angle decreases (). The finding may be explained using Fig. 2.4, which depicts the development of space charge within the sheath area. The magnetic field is nearly parallel to the z-axis in the instance of 89°. As a result, the ions have a growing tendency to gravitate towards the wall As a result, the sheath formation at this angle is identical to that of the electrostatic scenario. However, as soon as begins to decrease,

space charges build rapidly within a limited region of space. As a consequence, screening takes place over a shorter period of time as opposed to a longer period. α.

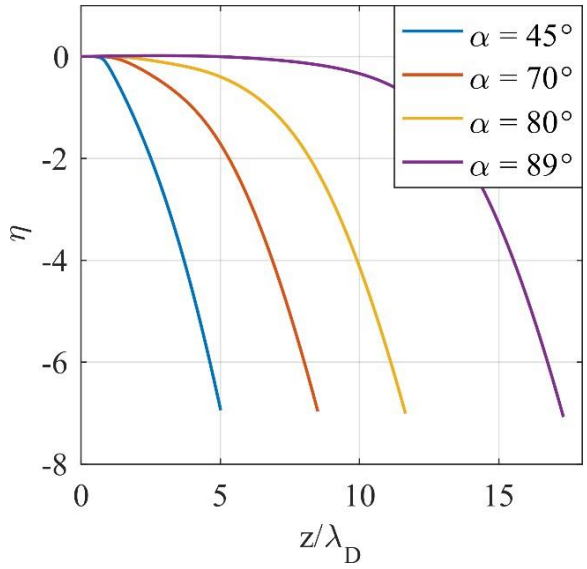

Fig. 2.2 The electric potential ($\boldsymbol{\eta}$) profiles at a magnetic field strength ($\boldsymbol{B}$) 4T.

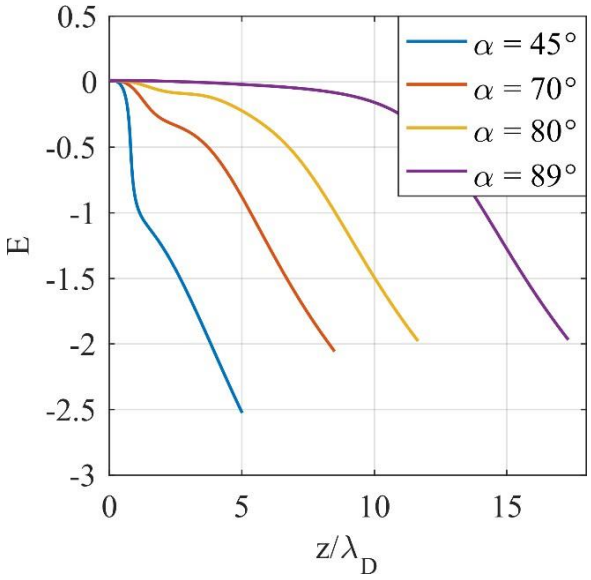

Fig. 2.3 The electric field ($\boldsymbol{E}$) profiles at a magnetic field strength ($\boldsymbol{B}$) 4T.

The development of ion density and velocity across a variety of angles is shown in Figures 2.5 and 2.6. At higher angles, the density map also indicates that the sheath development is similar in the electrostatic situation. By decreasing the value of, ion peaks emerge gradually. Furthermore, at greater angles, the B and E are almost parallel, causing the ions to travel at a faster rate along z. For = 89°, the other two components are determined to be zero. The magnetic field, on the other hand, begins to influence the situation as the angle increases,

and the other two components of velocity, u and v, share the net velocity at a point with w. The u component competes with w substantially in the extreme low case, = 45°..

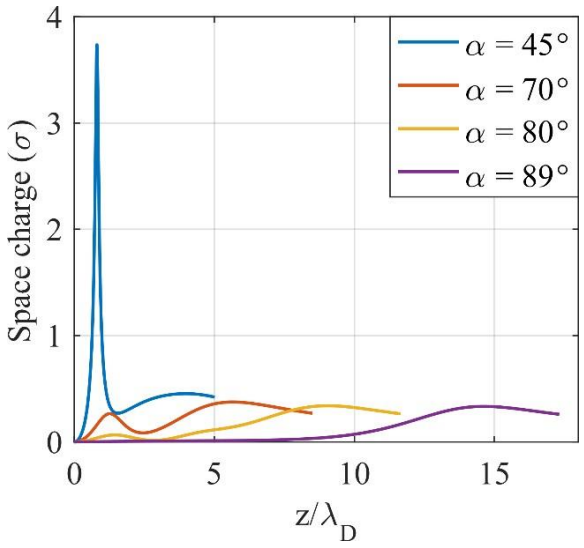

Fig. 2.4 The space charge (***σ***) profiles at a magnetic field strength (***B***) 4T.

A three-dimensional plot of the u, v, and w is shown in Fig. 2.7. Even in 3D velocity space, a helix may be observed evolving. With decreasing, the number of helix twists reduces. The helix widens out from above for greater angles and barely completes a single turn beyond that. This clearly demonstrates that at higher angles towards the wall, the w section governs and the supplementary two lose importance.

The computation of the terrain angle, which is the angle amid the element rapidity course and the attractive field, is regarded a crucial parameter in magnetic geometry. The angle is determined by,

$\theta = \tan^{-1}(\frac{v_{perp}}{v_{para}})$, where, $v_{perp} = \sqrt{(w\cos(\alpha) - u\sin(\alpha))^2 + v^2}$ and $v_{para} = u\cos(\alpha) + w\sin(\alpha)$.

The perpendicular component vperp is in charge of particle rotation around the

magnetic field, while the parallel component (vpara) is in charge of providing it a jump in the magnetic field's direction. The plot of the pitch angle against distance along z is shown in Fig. 2.8. For higher angles, the figure displays highly regular periodic patterns; but, when the angle is reduced, the regular periodic behaviour is lost. It's worth noting that the greatest amplitude occurs at the angle (90), i.e. the angle between the magnetic field and the ground. the *z*-axis.

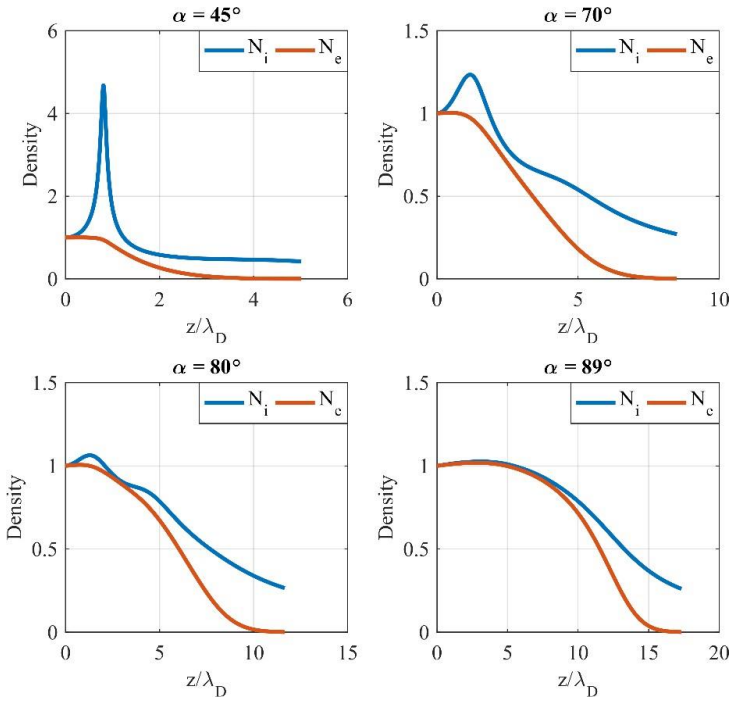

Fig. 2.5 The density distributions at a magnetic field strength (***B***) 4T.

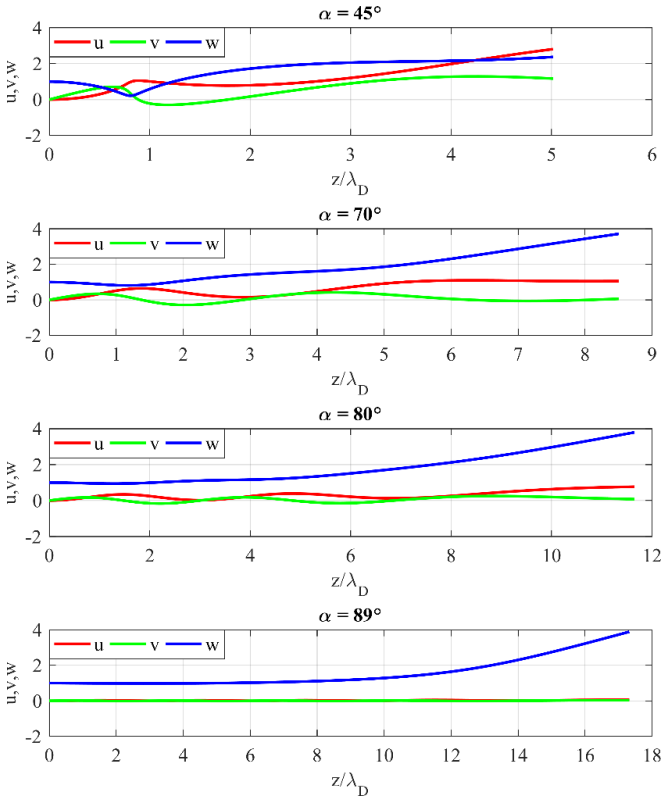

Fig. 2.6 The ion flow velocity components at a magnetic field strength (***B***) 4T.

As a result, pitch length is relative to the velocity's parallel constituent. The terrain length indicates how far the atom has leapt ahead as it spins around the magnetic field. The precise particle track is unclear in this work, therefore the velocity field construct with components is used instead. As a result, the pitch length here denotes P′, which would be the pitch length if the particle rotated in a continuous magnetic field at vpara. However, since the parallel velocity varies due to the action of the electric field, a unceasing development of pitch length is produced. The length, on the other hand, seems to be increasing along z in the development. For the higher angle, the pitch length stays relatively constant at first, before rising as it gets closer to the wall. This is observed to grow from the beginning for the lower angle..

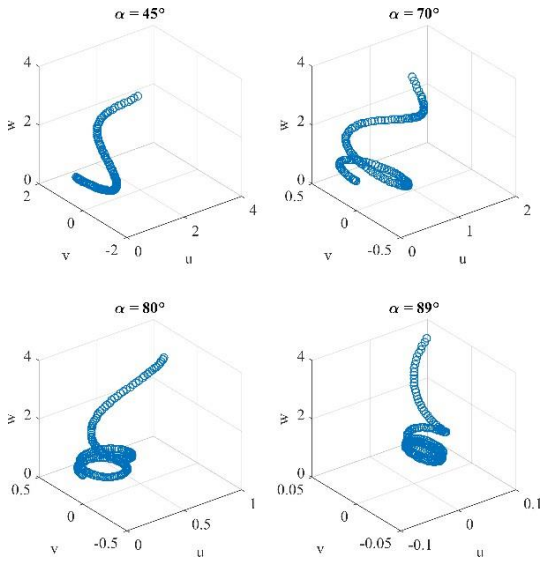

Fig. 2.7 The ion flow velocities at a magnetic field strength (***B***) 4T

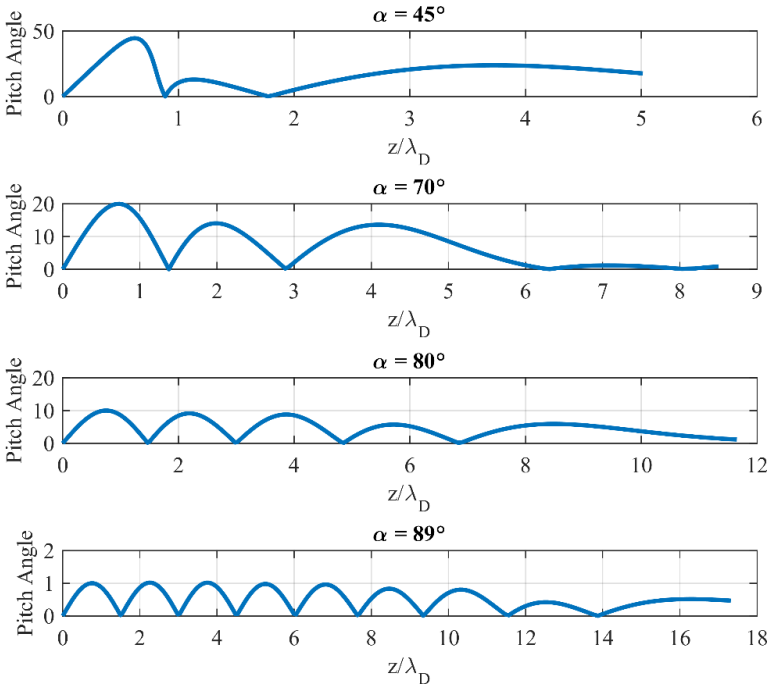

Fig. 2.8 The ion pitch angle profiles at a magnetic field strength (***B***) 4T.

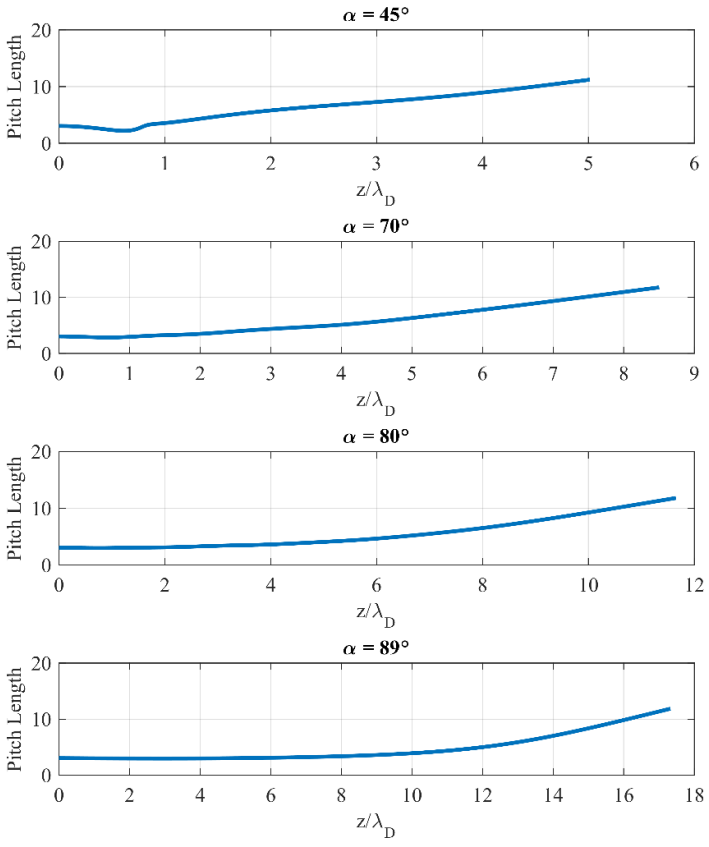

Fig. 2.9 The ion pitch length profiles at a magnetic field strength (***B***) 4T.

Conclusions

In the attendance of an angled magnetic field, this revision sheds light on the impact of force. The study of particle dynamics is always fascinating since it reveals a wealth of information about diverse magnet systems. The findings back with the theory that as the inclination angle decreases, the sheath width becomes less and smaller. It has been found that when the value of varies, the electric field profile becomes more scattered. When considering the effects on the recycling of sputtered particles at a tokamak edge, the dispersion of the electric field with decreasing is very significant. There is room to investigate the impact of the above-mentioned information. The formation of a peak in the ion density distribution as the value of decreases shows that ions are decelerating towards the wall owing to magnetic force. Due to the lower inclination angle, the periodicity of pitch angle is broken, resulting in a different impression of ion movement within the sheath. Despite the fact that the magnetic field is homogeneous across the domain, the pitch length paints a different image than normal. The Lorentz force analysis is very useful in understanding and explaining the dynamic behaviour of the ions in the system. While researching, the impact of magnetic field strength also exhibits some intriguing behaviour. While kinetic analysis offers a comprehensive view of particle dynamics, the current fluid analysis provides a comprehensive picture of such systems. Finally, using a fluid approach, this work offers up a new avenue for understanding ion dynamics within the sheath in the presence of a magnetic field.

REFERENCES

[1] N.A. Krall, and A.W. Trivelpiece, *Principles of Magnet Physics*, (McGraw-Hill, 1973).

[2] W.M. Stacey, *Fusion Magnet Physics*, (Wiley-VCH Verlag GmbH, 2005).

[3] P.C. Stangeby, *The Magnet Boundary of Magnetic Fusion Devices*, (CRCPress, 2000).

[4] J.A. Bittencourt, *Fundamentals of Magnet Physics*, Third, (Springer New York, 2004).

[5] P.M. Bellan, *Fundamentals of Magnet Physics*, (Cambridge University Press, 2006).

[6] R. Goldston, and P.H. Rutherford, *Introduction to Magnet Physics*, (Institute of Physics Publishing, 1995).

[7] M.A. Lieberman, and A.J. Lichtenberg, *Principles of Magnet Discharges and Materials Processing*, (John Wiley & Sons, Inc., 2005).

[8] T. Gyergyek, and J. Kovačič, Phys. Magnets. **22**, 43502 (2015).

[9] K.-U. Riemann, Contrib. Plasm. Phys. **34**, 127–132 (1994).

[10] N. Sternberg, and J. Poggie, IEEE Trans. Magnet Sci. **32**, 2217–2226 (2004).

[11] R.N. Franklin, J. Phys. D. Appl. Phys. **38**, 3412–3416 (2005).

[12] T.M.G. Zimmermann, M. Coppins, and J.E. Allen, Phys. Magnets. **16**, 43501 (2009).

[13] J.P. Freidberg, *Magnet Physics and Fusion Energy*, (Cambridge University Press, 2007).

[14] I.N. Ivchenko, S.K. Loyalka, and R. V Tompson, eds., The Free-Molecular Regime, in: Anal. Methods Probl. Mol. Transp., Springer Netherlands, 2007: pp. 91–140.

[15] D. Bohm, The Characteristics of Electrical Discharges in Magnetic Fields, in: A. Guthry, and R.K. Wakerling (Eds.), Charact. Electr. Discharges Magn. Fields, McGraw-Hill, 1949: p. 77.

[16] F.F. Chen, *Introduction to Magnet Physics and Controlled Fusion*, Second, (Springer India, 2012).

[17] L. Oksuz, and N. Hershkowitz, Magnet Sources Sci. Technol. **14**, 201–208 (2005).

[18] R. Chodura, Phys. Fluids. **25**, 1628 (1982).

[19] K.U. Riemann, Phys. Magnets. **1**, 552 (1994).

[20] P.C. Stangeby, Phys. Magnets. **2**, 702 (1995).

[21] E. Ahedo, Phys. Magnets. **4**, 4419–4430 (1997).

[22] I.I. Beilis, and M. Keidar, Phys. Magnets. **5**, 1545–1553 (1998).

[23] S. Devaux, and G. Manfredi, Phys. Magnets. **13**, 83504 (2006).

[24] F. Valsaque, and G. Manfredi, J. Nucl. Mater. **293**, 763–767 (2001).

[25] D. Tskhakaya, and S. Kuhn, J. Nucl. Mater. **313**–**316**, 1119–1122 (2003).

[26] D. Tskhakaya, and S. Kuhn, Magnet Phys. Control. Fusion. **47**, A327–A337

(2005).

[27] K.-U. Riemann, J. Phys. D. Appl. Phys. **24**, 493–518 (1991).

[28] R.N. Franklin, J. Phys. D. Appl. Phys. **37**, 1342–1345 (2004).

[29] R.N. Franklin, J. Phys. D. Appl. Phys. **36**, R309–R320 (2003).

[30] V.A. Godyak, and N. Sternberg, IEEE Trans. Magnet Sci. **18**, 159–168 (1990).

[31] K.-U. Riemann et al., Magnet Phys. Control. Fusion. **47**, 1949–1970 (2005).

[32] K.-B. Persson, Phys. Fluids. **5**, 1625 (1962).

[33] M. Warrier, R. Schneider, and X. Bonnin, Comput. Phys. Commun. **160**, 46–68(2004).J. Bohdansky, Nucl. Instruments Methods Phys. Res. Sect. B Beam Interact.with Mater. Atoms. **2**, 587–591 (1984).

[34] W. Eckstein, and R. Preuss, J. Nucl. Mater. **320**, 209–213 (2003).

[35] Y. Yamamura, Y. Itikawa, and N. Itoh, *Report on Angular dependence ofsputtering yields of monoatomic solids*, (1983).

[36] W. Eckstein, *Sputtered Energy Coefficient and Sputtering Yield*, (2011).

[37] ITER Physics Basis Editors et al, Nucl. Fusion. **39**, 2137–2174 (1999).

[38] A.S. Kukushkin et al., Fusion Eng. Des. **65**, 355–366 (2003).

[39] S. Devaux, and G. Manfredi, Magnet Phys. Control. Fusion. **50**, 25009 (2008).

[41] G.F. Matthews et al., Nucl. Fusion. **31**, 1495–1509 (1991).

[42] S.D. Baalrud, and C.C. Hegna, Magnet Sources Sci. Technol. **20**, 25013 (2011).